International Journal of Marine Engineering Innovation and Research, Vol.10, June 2025. 551-567
(pISSN: 2541-5972, eISSN: 2548-1479)

Fatigue Life Analysis Of Car Deck Construction on a Ferry Ro Ro

Amam Baharullah[1], Achmad Baidowi[2] and Edi Jadmiko[3]

(Received: 11 May 2025 / Revised: 17 June 2025 /Accepted: 23 June 2025 / Available Online: 30 June 2025)

***Abstract*— Fatigue life analysis is often overlooked in ship development, leading to an uncertain understanding of a ship's construction lifespan. This study focuses on the fatigue life of the car deck, which is affected by deformation on a ro-ro ferry. The research aims to determine the maximum stress, location, the cause of deformation, and the fatigue life of the car deck on a ro-ro passenger ship. The calculations assess the car deck's lifespan and provide a reference for future design considerations. Finite element analysis (FEA) is used, with fatigue life calculated using the Sonderberg method. The research begins with calculating the ship's weight and buoyancy distribution, then determining the ship's longitudinal strength from the load distribution. The analysis reveals that the highest stress occurs under hogging wave conditions, exceeding the yield strength of 321 MPa. Specifically, at overload and hogging wave conditions, the highest stress of 486.1 MPa is found on the starboard side between longitudinal stiffeners 1 and 2 (900 mm from the centerline), between frames 56 and 57, with a fatigue life of 4.3 years.**

Keywords—Car Deck Construction, Fatigue Life, Passengers Ship, Finite Element Method,

I. INTRODUCTION

Indonesia, the world's largest archipelagic nation, with 62.5% of its area covered by ocean, relies heavily on maritime transport to support its national logistics and economy. Passenger vessels, especially in regions inaccessible by land or air, play a crucial role in facilitating the mobility of people and goods across the archipelago. The 2022 Maritime Transport Statistics report that 25 strategic ports across 21 Indonesian provinces handle significant passenger volumes, highlighting the high demand for sea transport [1]. However, Indonesia's passenger ferries, particularly Ro-Ro vessels, have been involved in numerous accidents. Between 2019 and 2023, the Indonesian National Transportation Safety Committee (KNKT) recorded 76 incidents, including sinking, fires, and collisions. Technical issues, such as vessel age and inadequate maintenance, were identified as the primary causes [2]. Approximately 60% of Indonesia's fleet is over 20 years old, with 40% of vessels aged between 20 and 30 years and 20% exceeding 30 years [2]. This aging fleet raises concerns about the reliability and safety of these vessels, particularly in key structural areas like the car deck of passenger ferries.

Despite the downward trend in maritime accidents in Indonesia between 2019 and 2023, technical factors continue to be the leading causes of accidents. These technical factors include ship construction quality, vessel age, and inadequate maintenance [3]. Structural deformation, particularly in the car deck area, has been observed due to uneven load distribution and excessive vehicle weight. Vessels operating on the Gili Manuk route show an average overload of 32%, emphasizing the urgent need for fatigue life assessments to ensure the vessel's structural integrity and long-term reliability [4]. Data from the Indonesian National Shipowners Association (INSA) indicates that approximately 40% of ships in Indonesia are between 20 and 30 years old, and 20% are even over 30 years old. This means that 60% of vessels in Indonesia are considered old, with declining physical conditions and performance. This increases the likelihood of technical damage that may trigger accidents. The age of the vessels is a significant factor because older ships require more intensive maintenance, and without adequate care, the risk of accidents is higher [5]. Fatigue life analysis is essential to predict a vessel's lifespan, helping to anticipate potential maritime accidents that could result in fatalities. Additionally, such calculations are vital for ensuring safer operations and guide shipowners in planning operations to avoid losses[6], [7]. Fatigue life analysis is essential to prevent accidents and ensure the vessel's long-term operational reliability.

Global maritime data reveals similar challenges. General cargo ships contribute to 23% of maritime accidents, while passenger ferries, including Ro-Ro vessels, account for 13%, a notably higher percentage than other ship types [8]. A comparison of global and Mediterranean accident data shows that older ships are more prone to accidents. Ships older than 30 contribute to just 4.5% of global accidents, while the Mediterranean region sees a higher percentage of accidents among ships over 30 years old, with 7.9% [8]. This emphasizes the need for better maintenance and structural analysis, especially in countries like Indonesia, where many vessels operate beyond their recommended lifespan.

Research on ship fatigue life, particularly for passenger ferries, is crucial to ensuring safety and extending the operational life of these vessels. Previous studies have focused on various ship types, including tankers, container ships, and ferries, emphasizing stress analysis and fatigue life prediction. For example, stress analysis on the car deck of a passenger ship under dynamic load var-

Amam Baharullah is with Departement of Marine Engineering, Institut Teknologi Sepuluh Nopember, Surabaya, 60111, Indonesia. E-mail : baharullahamam@gmail.com

Achmad Baidowi is with Departement of Marine Engineering, Institut Teknologi Sepuluh Nopember, Surabaya, 60111, Indonesia. E-mail: achmad.baidowi@its.ac.id

Edi Jadmiko is with Departement of Marine Engineering, Institut Teknologi Sepuluh Nopember, Surabaya, 60111, Indonesia. E-mail: e.djstmiko@yahoo.com

iation was conducted using the fatigue life Rule/Class method [6]. Research by Corigliano et al. (2020) and Misbah et al. (2018) focused on dynamic loads on container ships and barges [9], [10]. Fatigue life estimation methods like Sonderberg, Goodman, and Gerber under dynamic loading remain underexplored. However, a significant gap remains in the literature regarding the specific analysis of the car deck's fatigue life in passenger ferries, especially those operating in Indonesia's maritime environment. Many vessels operate without a proper understanding of fatigue life, increasing the risk of structural failures and accidents, particularly in older ships. This research aims to address this gap by using finite element analysis to examine the stress distribution and fatigue life of ferry car decks under various loading conditions, including overload scenarios and adverse sea states such as sagging and hogging. The novelty of this research lies in its detailed evaluation of the fatigue life of the car deck, especially under overloaded conditions and extreme wave states such as sagging and hogging [6]. This study will assess the structural integrity of the car deck, identify high-stress areas, and propose design optimizations to mitigate these stresses. The findings are expected to contribute significantly to the maritime industry, improving safety standards, reducing the risk of accidents, and extending the operational life of passenger ferries both in Indonesia and globally.

II. METHOD

This study focuses on a Ro-Ro ferry built by an Indonesian shipyard. The vessel was selected due to deck deformation caused by vehicle overloading after just one year of operation. Data were collected through direct observation, measurements from working drawings, and literature review. Various loading conditions were analyzed to identify fatigue stress points and estimate the vessel's fatigue life. The results were used to propose design improvements to enhance the durability of similar ships. The methodology comprises the following steps:

A. Ship Data

These ship specifications determine the structural characteristics and load conditions the car deck faces during the vessel's operation [11]. As a passenger vessel, the ship is designed to meet both safety regulations and operational requirements for domestic ferry services, including load capacity, stability, and efficient fuel usage [12]. The specification of the ferry Ro-Ro vessel used in this study are as follows:

TABLE 1.
SHIP SPECIFICATIONS

Ship Specifications		
LOA	63.75	m
LPP / LBP	57.23	m
B	13.60	m
H	3.90	m
T	2.80	m
Vs	12.00	knots
Vr	13.00	knots
Main Engine	2 x 1400	HP
ABK	20	person
Passenger	252	person
Medium Truck	18	units
Car	8	units
Shipping Area	Terbatas	
Ship Type	Ferry Ro Ro	Passenger

B. Load Calculation

The study assesses various loads acting on the vessel, including those from the structure, equipment, vehicle loads, and buoyancy forces. The loading conditions analyzed in this research include: Empty ship – calm water, Normal load – calm water, Overload – calm water, Empty ship – sagging, Normal load – sagging, Overload – sagging, Empty ship – hogging, Normal load – hogging, and Overload – hogging [13].

Each load condition is computed to determine the forces acting on the ship's structure, which are then used for strength analysis and fatigue life prediction [14].

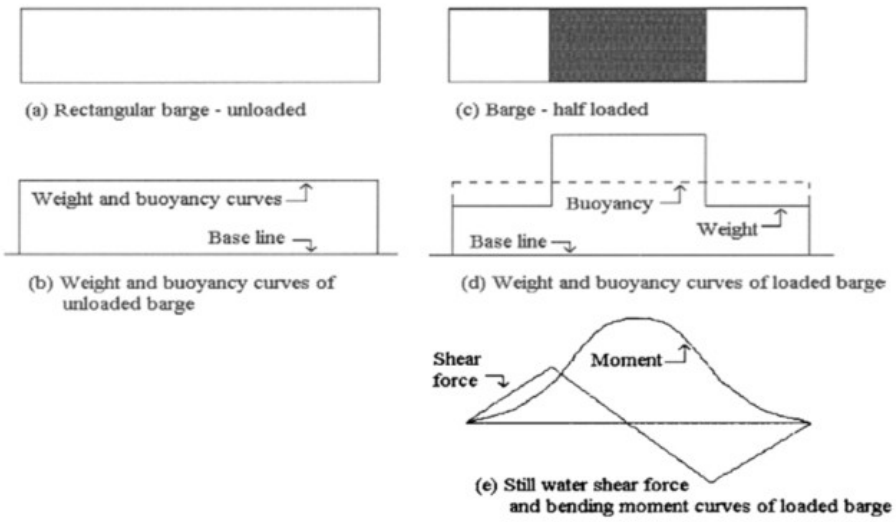

Figure. 1. Bending Moment Changes on a Rectangular Barge in Calm Water Conditions [13]

C. Wave Calculation

Wave calculation in this study follows the guidelines set by the Indonesian Classification Bureau [15], Volume II, Section 1.D.6 : Ship – sagging, Normal load–sagging, Overload – sagging, Empty ship–hogging, Normal load – hogging, and Overload – hogging [13].

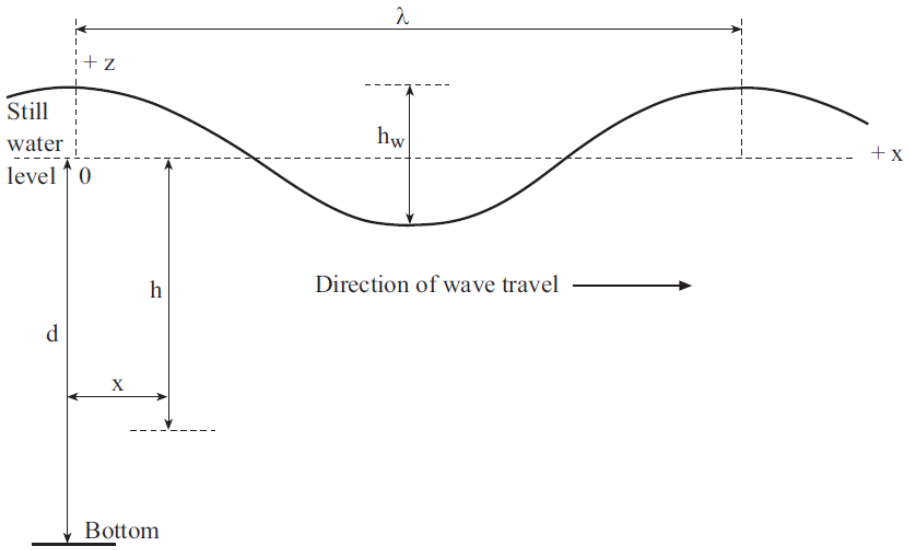

Figure. 2. Wave Calculation by BKI [15]

Surface Wave Profile

$$z = 0.5\, h_w \cos(kx - \omega t) \;\; where\, d > \lambda/2 \quad (1)$$

Water Particle Velocity for Deep Water Waves

Horizontal

$$V_x = 0.5.\omega.h_w.e^{-kh}.cos(k.x - \omega.t)\ [^m/_s] \quad (2)$$

Vertikal

$$V_z = -0.5.\omega.h_w.e^{-kh}.sin(k.x - \omega.t)\ [^m/_s] \quad (3)$$

The wave propagates along the horizontal x-axis.

Water Particle Acceleration for Deep Water Waves

Horizontal

$$a_x = 0.5.\omega.h_w.e^{-kh}.\sin(k.x - \omega.t)\ [^m/_s] \quad (4)$$

Vertical

$$a_z = -0.5.\omega.h_w.e^{-kh}.\cos(k.x - \omega.t)\ [^m/_s] \quad (5)$$

Wave Pressure

$$\rho = 0{,}5.\mathrm{p.g.}\,h_w.e^{-kh}.\cos(k.x - \omega.t) \quad (6)$$

Where ρ is the water density, g is the acceleration due to gravity, and h_w is the wave height [15]

D. Ship Strength Calculation

After calculating the loads acting on the vessel, structural strength analysis is conducted to identify bending moments, shear forces, and deflections under sagging and hogging conditions [10].

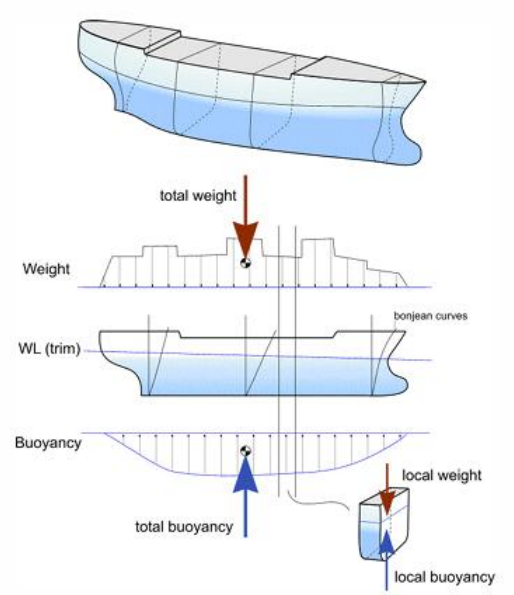

Figure. 3. llustration of Ship Strength Calculation [14]

Using beam theory, the hull is modeled as a beam under distributed loads to evaluate longitudinal stress and detect fatigue-critical areas using the formula [14] :

$$V(X) = \int_0^X b(x) - w(x)dx \quad (7)$$

Where *b(x)* and *w(x)* represent buoyancy force and weight at location x, respectively. The bending moment at location *X*, *M(X)* is the integral of the shear force curve [16]. These equations help evaluate critical regions under hogging and sagging conditions [17].

$$M(X) = \int_0^X V(x)dx \quad (8)$$

E. *Car Deck Construction Modeling*

The car deck structure is modeled using FEM software to accurately represent real-world conditions. Components such as the car deck, mainframe, web frame, deck beams, longitudinals, center girders, side girders, brackets, and plate rows are modeled [18]. The material properties of structural steel are assigned to the model, and stress analysis is performed. Results include the stress distribution and identification of critical points for further interpretation [19], [20].

F. Support and Loading

Support positions and load applications follow theoretical principle in figure 4. Supports are strategically placed at specific points on the structure, while loads are applied at other areas. These placements are based on established mechanical theories, ensuring the model reflects realistic boundary conditions [20], [21]. The boundary settings are configured to simulate longitudinal deformation due to varying wave conditions [22].

Figure. 4. Support and Loading on a Specific Section [20]

G. Stress Analysis

Stress analysis identifies the maximum stress and distribution across the vessel's frame. Von Mises stress is evaluated against the material's yield and ultimate tensile strengths to assess potential deformation risks. This

analysis helps identify areas vulnerable to failure due to fatigue [23].

H. Convergence

Convergence testing is performed to ensure the accuracy of the finite element model by determining the optimal element size in the mesh. Stress results are compared across different mesh variations until the results stabilize. Mesh metric values are used to assess the convergence of the model, ensuring the reliability of the analysis results in Figure 5 [24].

Figure. 5. Skewness and orthogonal quality mesh metrics spectrums [24]

I. Fatigue Life Calculation

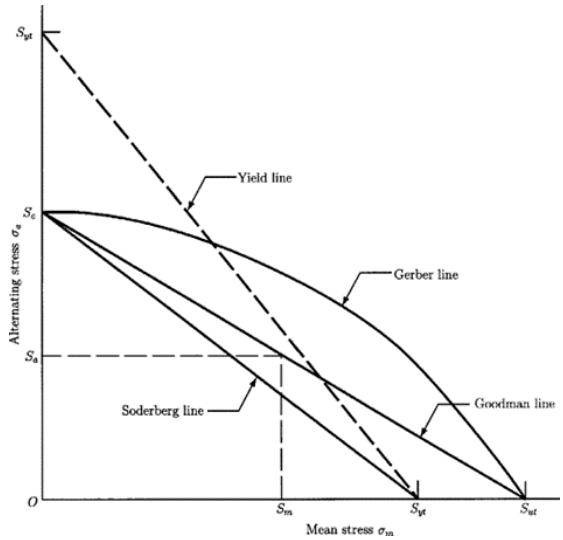

Figure. 6. Material Stress Fatigue Limit Diagram [25]

Fatigue life is calculated using the S-N (Wöhler) curve, which correlates the stress range to the number of cycles until failure. This curve, along with the Goodman, Sonderberg, and Gerber diagrams, is utilized to assess the effect of mean stress on the fatigue life of materials. Several conclusions can be drawn based on the comparative analysis of these diagrams. First, the Soderberg Diagram (a) represents the most conservative and safest criterion, particularly when the stress ratio (R) approaches 1. The Goodman Diagram (b) and Gerber Diagram (c) typically represent experimental data, falling between the conservative Soderberg and the more aggressive Morrow criteria. The Goodman and Morrow diagrams (diagrams b and d) yield similar results for brittle steels. Morrow's diagram (d) offers a more accurate prediction of fatigue life for ductile steels. Finally, when

R < 1 or the difference between mean stress and amplitude is minimal, all four criteria provide comparable results. An alternative Goodman diagram is also included to offer flexibility for various material behaviors [25], [26]. An alternative Goodman diagram is also illustrated in Figure 6.

III. RESULTS AND DISCUSSION

A. Block Construction Weight Calculation

The car deck is subjected to load pressure and bending moments induced by block construction loads. Load calculations are based on the construction section detailed in the production drawing. The complete calculation results are presented in Table 2.

TABLE 2.
BLOCK CONSTRUCTION WEIGHT

Block Construction Weigth Calculation								
No	Block - 01	Weigth (Ton)	Block - 02	Weigth (Ton)	Block - 03	Weigth (Ton)	Block - 04	Weigth (Ton)
1	112 – 01	31.62	112 – 02	3.98				
2	113 – 01	33.23	113 – 02	10.89				
3	114 – 01	38.24	114 – 02	19.38	114 – 03	15.94		
4	115 – 01	36.98	115 – 02	18.21	115 – 03	9.43	115 – 04	1.68
5	116 – 01	41.46	116 – 02	15.21	116 – 03	5.76	116 – 04	4.58
6	117 – 01	42.14	117 – 02	18.67	117 – 03	11.89	117 – 04	7.49
7	118 – 01	36.79	118 – 02	18.03	118 – 03	18.21	118 – 04	10.62
8	119 – 01	33.34	119 – 02	17.26	119 – 03	12.20	119 – 04	9.11
9	120 – 01	33.23	120 – 02	18.20	120 - 03	12.71	120 - 04	13.08
10	121 – 01	21.92	121 – 02	14.46				
11	122 – 01	19.14	122 - 02	7.22				
12	123 – 01	11.67						
Total Block Construction Weigth Calculation					673.97		Ton	

B. Vehicle Weight Calculation

Figure 7 illustrates load points on the car deck under normal and overload conditions based on the vehicle placement plan.

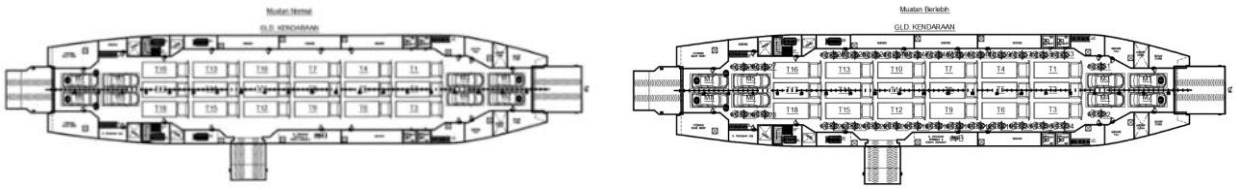

(a) Normal Load Vehicle Load (b) Overload Vehicle Load

Figure. 7. Vehicle Load Conditions Schema

Referring to the general arrangement, vehicle loads consist of trucks, cars, and motorcycles. The truck is a class two truck with three axles, carrying a total weight of 18 tons, distributed as 7 tons at the front (2 wheels) and 11 tons at the rear (8 wheels). The motorcycle example is an Nmax model, with a total weight of 0.25 tons and a load distribution of 50% at both the front and rear. The car example is an Avanza, with a total weight of 1.1 tons and an equal load distribution of 50% at the front and rear.

TABLE 3.
VEHICLE WEIGHT CALCULATION

Vehicle Weigth Calculation						
Normal Vehicle Load Condition Schema						
No	Vehicle	Weigth (Ton)	Front Axle (Ton)	Rear Axle(Ton)	Number of Vehicles	Total Weigth (Ton)
1	Truck	18	7	11	18	324
2	Car	1.1	0.55	0.55	8	8.8
3	Motorcycle	0.179	0.0895	0.0895	0	0
				Total	26	333
Overload Vehicle Load Condition Schema						
No	Vehicle	Weigth (Ton)	Front Axle (Ton)	Rear Axle(Ton)	Number of Vehicles	Total Weigth (Ton)
1	Truck	23.76	9.24	14.52	18	428
2	Car	1.1	0.55	0.55	8	8.8
3	Motorcycle	0.179	0.0895	0.0895	30	5.37
				Total	56	442

The resulting loads are presented in Table 3. In overload conditions, the load increases by 32%, based on a 2020-2021 survey using the Gilimanuk-Bali crossing as a sample for overload. The total load schema for these overload conditions is detailed in Table 3.

	June	July	August	Spetember	October	November	December	January	February	April	March	May	June
Average Load per Trip (tons)	116.36	109.33	95.94	105.70	103.32	97.73	85.01	83.40	99.66	93.28	108.44	101.92	102.75
Max DWT	81.7	81.7	81.7	81.7	81.7	81.7	81.7	81.7	81.7	81.7	81.7	81.7	81.7
Trip	85	97	107	169	104	123	56	162	141	161	141	132	131

Figure. 8. Average Loading on the Gilimanuk – Bali

C. Engine, Equipment, and Tank

Ships are subjected to load pressure due to the weight of machinery, equipment, and tanks installed on board. The load calculation refers to the specifications and data provided by the shipyard responsible for building KMP Aceh Hebat 2. Table 4 presents the total load of the machinery, equipment, and tanks.

TABLE 4.
ENGINE, EQUIPMENT AND TANK

Block Construction Weigth Calculation								
No	Equipment		Propultion		Engine		Tank	
	Part	Weigth (Ton)	Part	Weigth (Ton)	Part	Weigth (Ton)	Part	Weigth
1	Windlass 1	0.417	Proppeller	0.449	Main Engine 1	16.8	FWT 1	137
2	Windlass 2	0.417	Main Shaft	0.87	Main Engine 2	16.8	FWT 2	137
3	Windlass 3	0.56	Inter. Shaft	0.089	M. Genset 1	4.417	FWT 3	15.8
4	Windlass 4	0.56			M. Genset 2	4.417	FOT 1	130.3
5	Anchor 1	0.923			M. Genset 3	4.417	FOT 2	130.3
6	Anchor 2	0.923			M. Genset 4	4.417	LOT 1	6.1
7					Emerg. Genset	2.991	LOT 2	6.1
8							Sludge Tank	9.8
9							Bilge Tank	9.8
Total Weigth Engine, Equipment and Tank					631.867		Ton	

D. Calculation of Weight Distribution

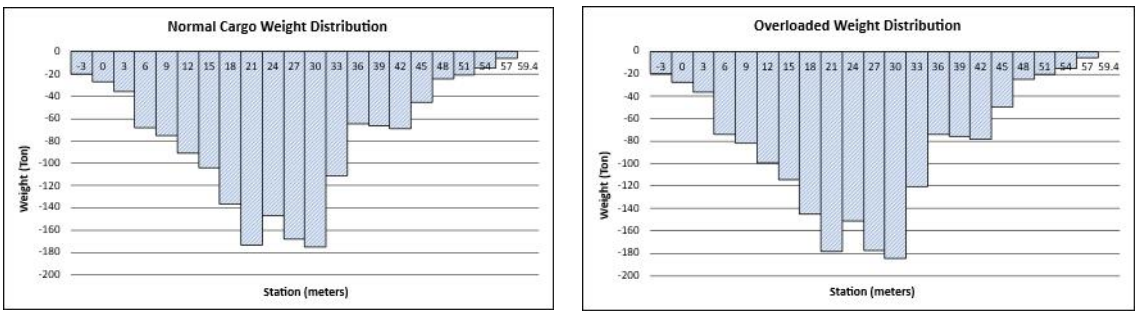

(a) Normal Loading Condition (b) Overload Loading Condition

Figure. 9. Ship Weight Distribution

E. Wave Calculation

The wave calculation adheres to BKI Vol II 2011, Section 1 on “Environmental Conditions.” The buoyancy curves generated for sagging and hogging wave conditions are presented for each load condition.

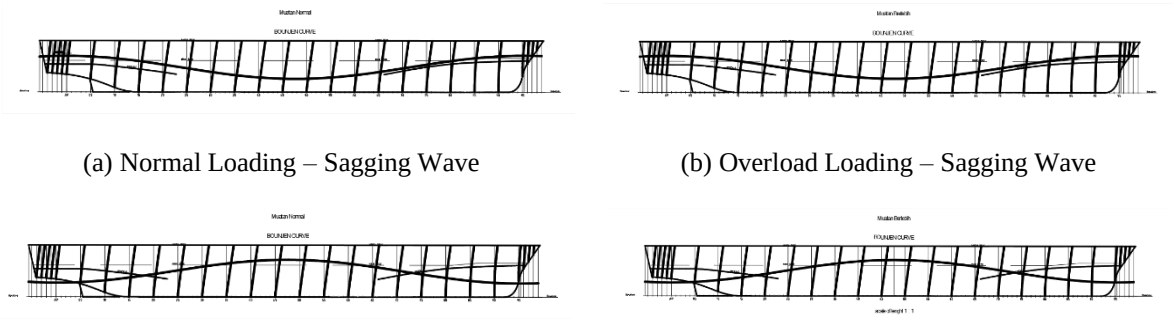

(a) Normal Loading – Sagging Wave (b) Overload Loading – Sagging Wave

(c) Normal Loading – Hogging Wave (d) Overload Loading – HoggingWave

Figure. 10. Bounjen Curve Loading and Wave Condition

F. Calculation of Bouyancy Distribution

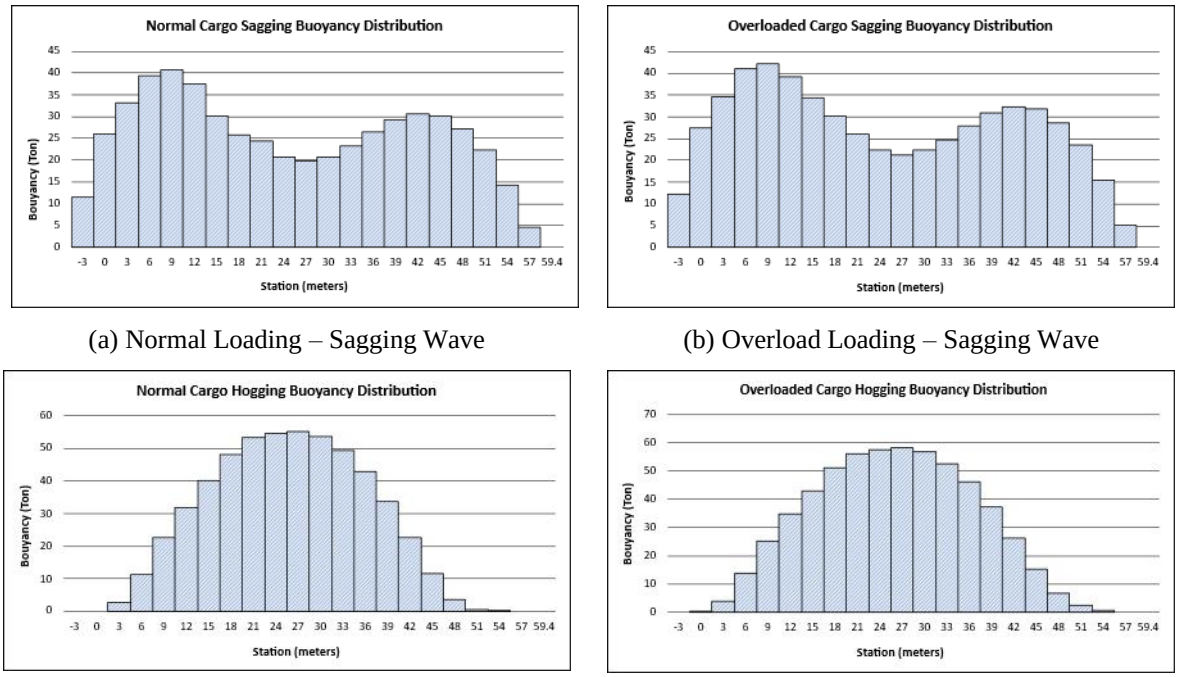

(a) Normal Loading – Sagging Wave (b) Overload Loading – Sagging Wave

(c) Normal Loading – Hogging Wave (d) Overload Loading – HoggingWave

Figure. 11. Bounjen Distribution Loading and Wave Condition

G. Calculation of Load Distribution

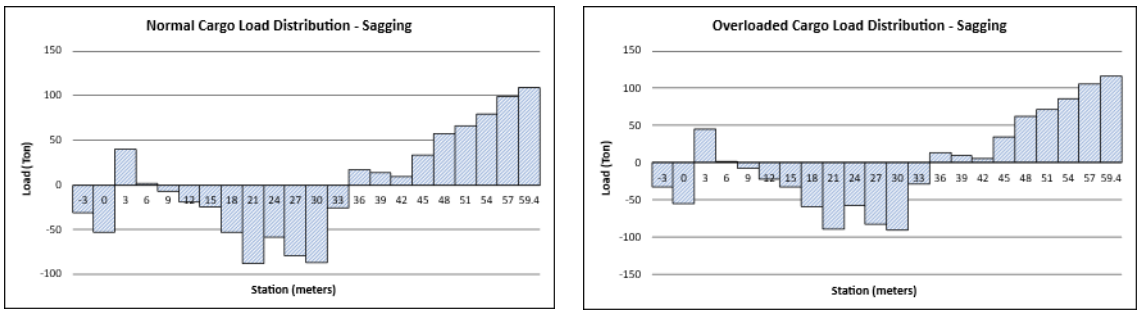

(a) Normal Loading – Sagging Wave (b) Overload Loading – Sagging Wave

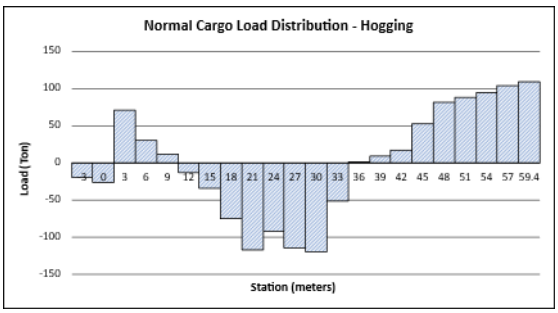

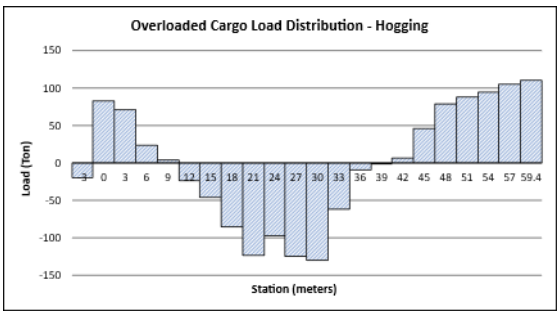

(c) Normal Loading – Hogging Wave (d) Overload Loading – HoggingWave

Figure. 12. Load Distribution Loading and Wave Condition

H. Bending Moment Calculation

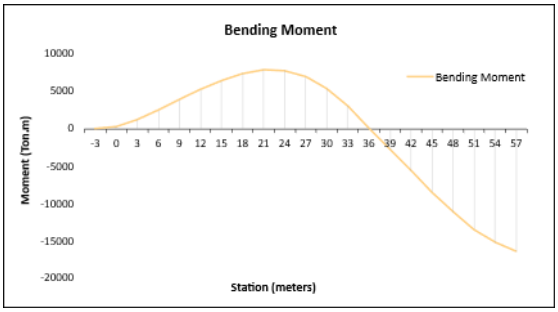

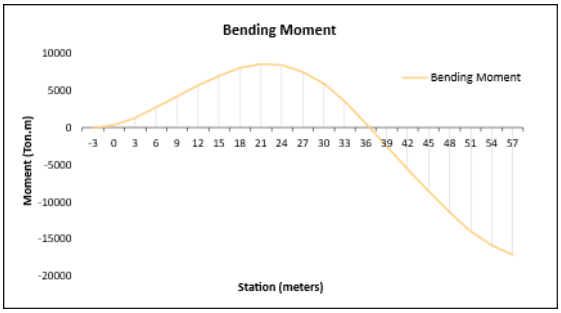

(a) Normal Loading – Sagging Wave (b) Overload Loading – Sagging Wave

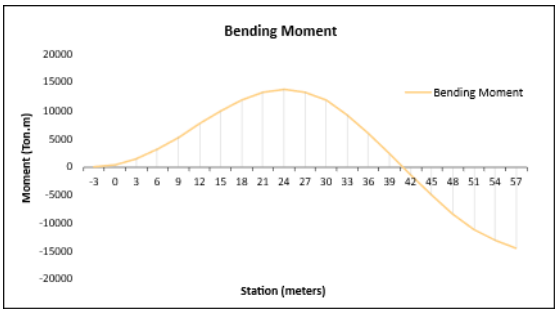

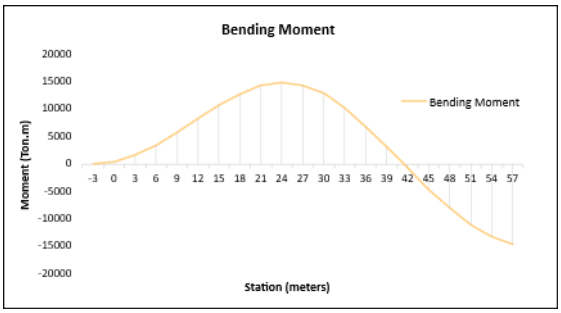

(c) Normal Loading – Hogging Wave (d) Overload Loading – HoggingWave

Figure. 13. Bending Moment Loading and Wave Condition

I. Modeling Selection

The model encompasses frames 49 to 58, focusing on blocks 118-01, as illustrated in Figure 1. This section, while not entirely modelled, reflects the critical and high-load areas of the car deck based on the production drawings and general arrangement.

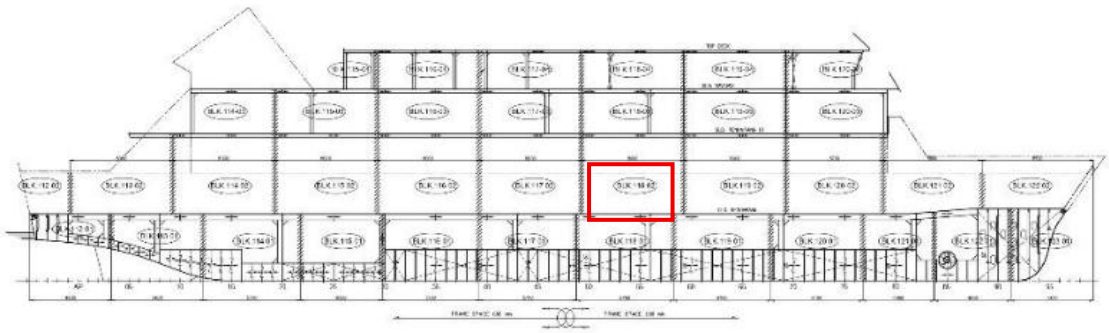

Figure. 14. Block Division Ferry Ro-Ro Ship

J. Engineering Data

The plate certificate designates grade A steel with Hot Rolled Steel Plate no. Heat Number 2962791 possesses the following material properties:

1) Yield Strength: 321 MPa.
2) Ultimate Strength: 432 MPa
3) Elongation Strength : 29%

K. Convergence and Meshing

The meshing size applied is 20 mm, which is deemed optimal based on convergence from the standard mesh quality. The mesh quality parameters consist of 1,078,323 elements, 2,162,945 nodes, a skewness value of 0.73584, and a 20 mm mesh size rated as "good" under the skewness parameter compared to other meshing, as presented in Table 5. Figures 15 illustrate the meshing results.

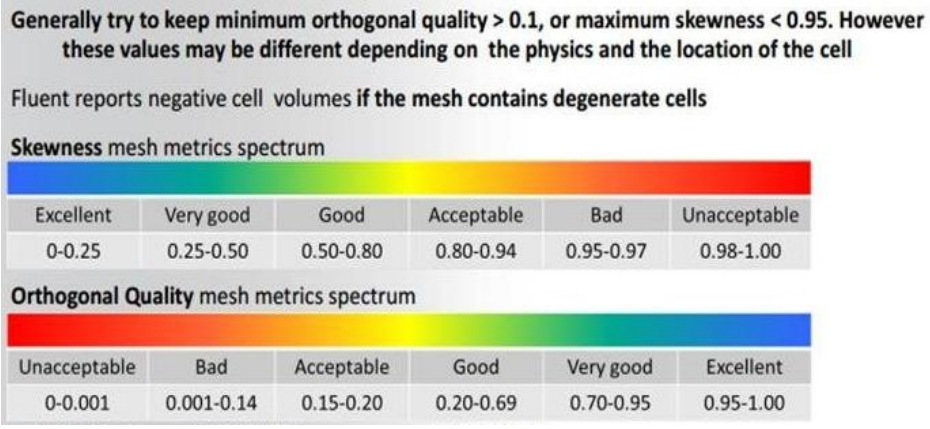

Figure. 15. Meshing Quality From Software [24]

TABLE 5.
CONVERGENCE

Convergence					
No	Meshing	Stress Max	Nodes	Element	Sqewness
1	70	499.2	990649	488901	0.856
2	65	503.5	1098551	543324	0.846
3	60	490.5	1150992	569661	0.840
4	55	495.9	1296425	642040	0.825
5	50	491.9	1379785	683666	0.819
6	25	494.8	1468988	731980	0.804
7	45	508.4	1664707	825233	0.791
8	30	480.5	1819955	904439	0.765
9	40	525.1	1850987	917894	0.770
10	20	523.3	2162945	1078323	0.735
11	35	538.2	2212266	1096604	0.744

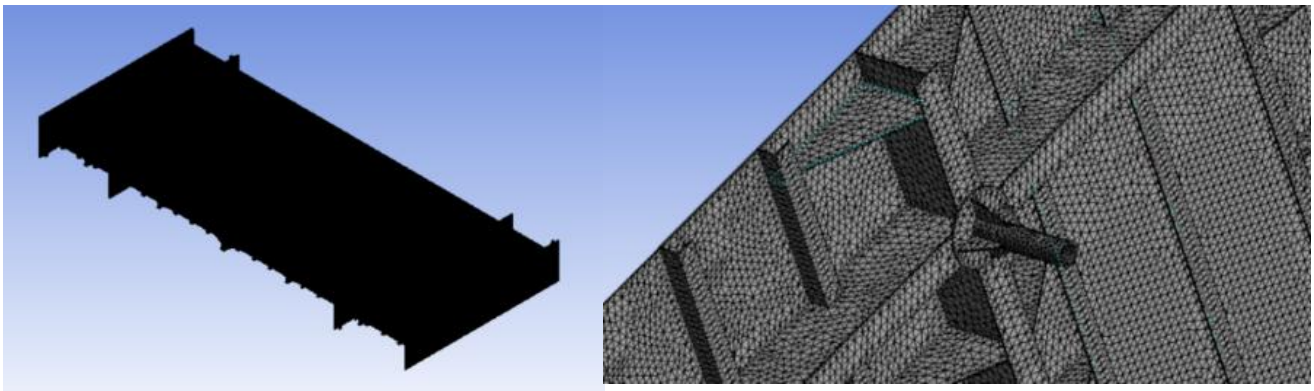

Figure. 16. Meshing 20 mm

L. Support and Loading

TABLE 6.
LOAD INPUT FROM SHIPS STREGTH

Load Input			
No	Condition	Bending Moment	
		Ton.m	N.m
	Normal Load		
1	Sagging	196.7	1928045.3
2	Hogging	5974.4	58549039.9
	Overload		
1	Sagging	597.1	5851218.3
2	Hogging	6863.5	67262127.8

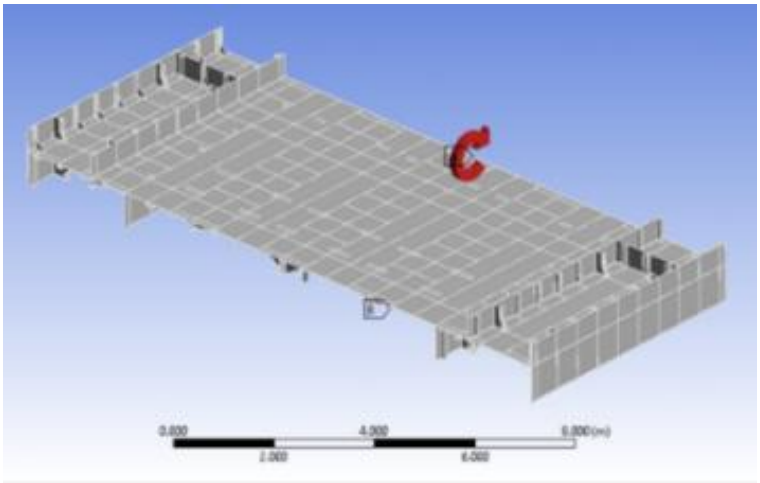

Figure. 17. Bending Moment Input Software

M. Stress Analysis

Figure 18 shows deformation between the truss and longitudinal reinforcements, prompting stress evaluation at the corresponding field-observed location.

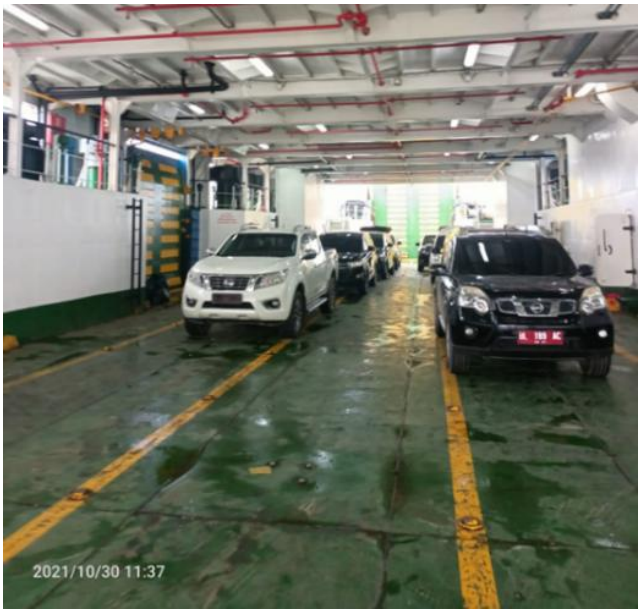

Figure. 18. Deformation in the Field

1) Normal Load Condition and Sagging Wave Condition

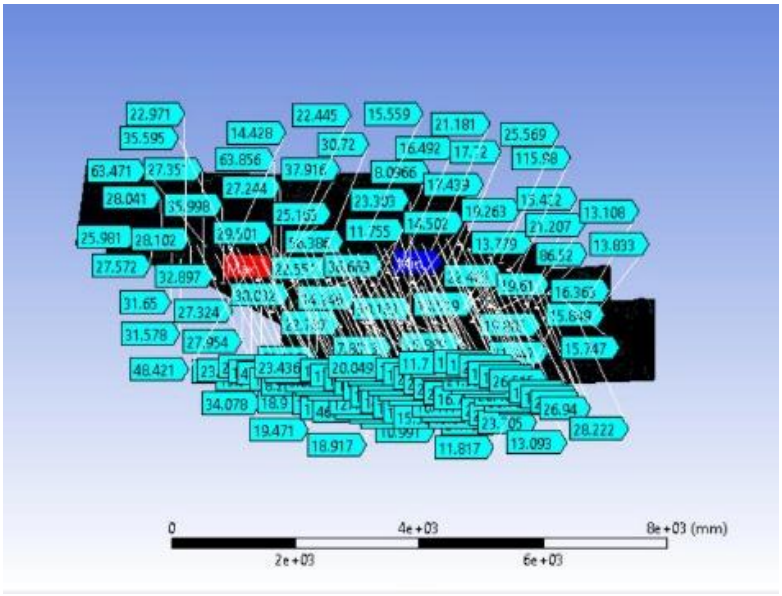

Figure. 19. Stress Distribution - Normal Load Condition and Sagging Wave Condition

TABLE 7.
STRESS DISTRIBUTION NORMAL LOAD CONDITION AND SAGGING WAVE CONDITION

Port Side Area Stress Distribution									
No	Frame	Port Side PS – from Centre Line (Mpa)							
		L6 – L7 4500 mm	L5 – L6 3900 mm	L4 – L5 3300 mm	T side – L4 2700 mm	L3 – T Side 2100 mm	L2 – L3 1500 mm	L1 – L2 900 mm	T centre – L1 300 mm
1	49 – 50	25.98	27.57	28.04	31.65	31.57	28.10	27.35	32.89
2	50 – 51	22.97	23.27	63.47	19.51	14.42	35.59	48.42	18.90
3	51 – 52	23.38	19.43	45.08	14.68	8.24	25.16	37.91	14.69
4	52 – 53	23.43	15.75	39.34	9.65	7.64	25.23	30.72	12.44
5	53 – 54	22.44	14.42	17.21	14.15	14.62	15.64	16.98	14.59
6	54 – 55	20.04	14.39	19.22	21.23	21.23	19.62	18.33	16.49
7	55 – 56	15.55	14.04	19.51	23.91	23.91	23.77	20.57	16.77
8	56 – 57	11.70	15.90	74.23	21.99	21.99	56.39	78.95	20.40
9	57 – 58	13.77	12.54	25.00	16.43	16.43	26.51	25.56	17.79
Starboard Area Stress Distribution									
No	Frame	Starboard SB – from Centre Line (Mpa)							
		T centre – L1 300 mm	L1 – L2 900 mm	L2 – L3 1500 mm	L3 – T Side 2100 mm	T side – L4 2700 mm	L4 – L5 3300 mm	L5 – L6 3900 mm	L6 – L7 4500 mm
1	49 – 50	35.99	27.32	27.95	30.99	34.07	29.50	27.24	30.03
2	50 – 51	18.88	63.85	56.38	14.24	19.47	65.62	22.55	22.78
3	51 – 52	15.48	46.21	36.66	7.80	11.75	58.18	18.91	23.09
4	52 – 53	13.39	27.44	23.95	8.09	10.99	39.59	15.88	23.30
5	53 – 54	15.00	17.01	15.55	14.50	14.51	17.43	14.46	22.40
6	54 – 55	16.41	18.72	19.84	21.75	21.08	19.26	13.77	19.88
7	55 – 56	17.72	22.23	24.08	23.70	21.34	19.61	13.09	15.44
8	56 – 57	20.70	126.21	115.98	22.07	21.20	86.52	15.84	11.81
9	57 – 58	17.73	28.05	26.94	16.36	15.74	28.22	13.10	13.88

2) Normal Load Condition and Hogging Wave Condition

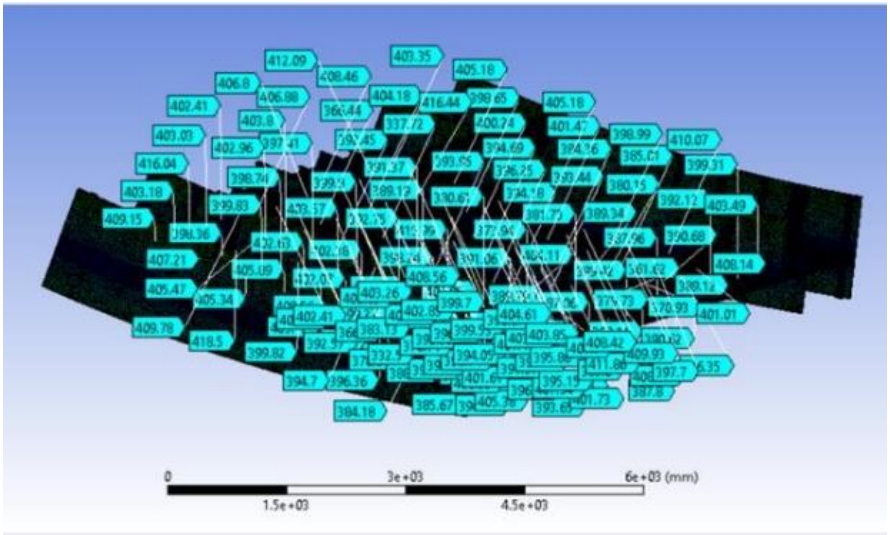

Figure. 20. Stress Distribution - Normal Load Condition and Hogging Wave Condition

TABLE 8.
STRESS DISTRIBUTION NORMAL LOAD CONDITION AND HOGGING WAVE CONDITION

Port Side Area Stress Distribution									
No	Frame	Port Side PS – from Centre Line (Mpa)							
		L6 – L7 4500 mm	L5 – L6 3900 mm	L4 – L5 3300 mm	T side – L4 2700 mm	L3 – T Side 2100 mm	L2 – L3 1500 mm	L1 – L2 900 mm	T centre – L1 300 mm
1	49 – 50	403.49	399.31	389.12	392.12	390.62	387.80	387.96	399.11
2	50 – 51	408.14	401.01	246.35	390.68	370.93	361.62	249.68	379.73
3	51 – 52	410.07	397.70	408.01	385.01	380.15	389.34	401.73	393.44
4	52 – 53	409.93	398.99	411.86	389.60	384.36	395.15	407.54	396.85
5	53 – 54	408.42	401.70	401.47	395.86	393.03	391.57	394.69	401.61
6	54 – 55	405.18	403.85	403.03	401.40	400.24	394.05	390.74	399.75
7	55 – 56	404.61	398.07	398.07	399.53	396.75	392.53	376.71	337.80
8	56 – 57	405.18	399.70	416.44	402.85	403.78	404.18	383.13	366.80
9	57 – 58	408.56	403.35	412.09	403.26	402.09	408.46	406.80	402.41
Starboard Area Stress Distribution									
No	Frame	Starboard SB – from Centre Line (Mpa)							
		T centre – L1 300 mm	L1 – L2 900 mm	L2 – L3 1500 mm	L3 – T Side 2100 mm	T side – L4 2700 mm	L4 – L5 3300 mm	L5 – L6 3900 mm	L6 – L7 4500 mm
1	49 – 50	399.42	386.81	387.06	390.86	391.81	389.79	399.84	402.72
2	50 – 51	381.73	356.09	367.21	373.94	391.06	341.72	401.95	406.82
3	51 – 52	393.65	404.11	394.18	380.61	385.67	415.99	398.24	409.85
4	52 – 53	396.25	405.38	396.15	384.18	389.19	414.39	399.27	409.30
5	53 – 54	400.39	393.95	391.37	392.75	396.36	402.38	402.07	408.56
6	54 – 55	399.17	388.14	394.70	399.80	403.57	403.12	402.63	405.89
7	55 – 56	332.50	378.80	392.45	397.41	399.82	398.74	399.83	405.34
8	56 – 57	366.44	392.57	403.80	402.96	405.47	418.50	398.36	407.21
9	57 – 58	403.81	406.88	409.78	402.41	403.03	416.04	403.18	409.15

3) Over Load Condition and Hogging Wave Condition

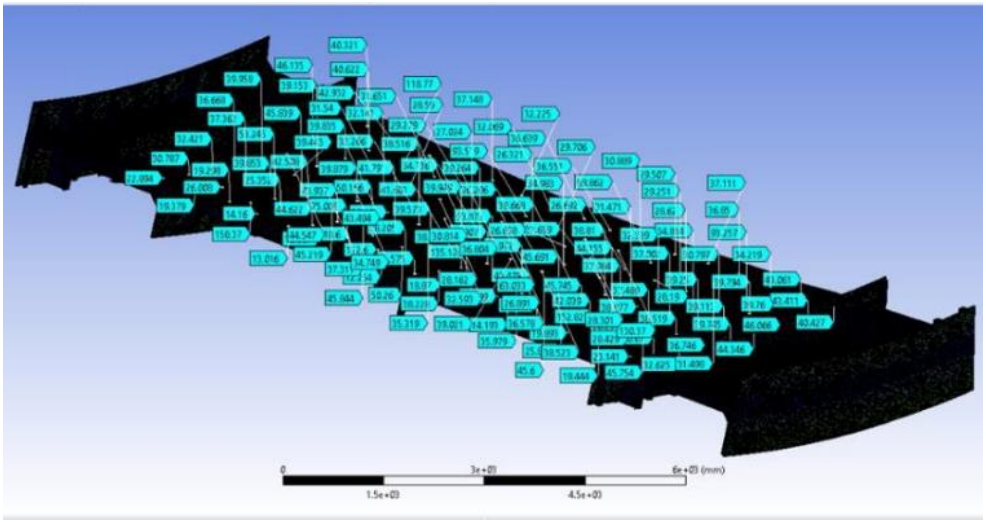

Figure. 21. Stress Distribution - Over Load Condition and Hogging Wave Condition

TABLE 9.
STRESS DISTRIBUTION OVER LOAD CONDITION AND SAGGING WAVE CONDITION

Port Side Area Stress Distribution									
No	Frame	Port Side PS – from Centre Line (Mpa)							
		L6 – L7 4500 mm	L5 – L6 3900 mm	L4 – L5 3300 mm	T side – L4 2700 mm	L3 – T Side 2100 mm	L2 – L3 1500 mm	L1 – L2 900 mm	T centre – L1 300 mm
1	49 – 50	22.89	19.37	19.29	14.16	13.01	16.86	18.60	12.25
2	50 – 51	30.78	26.00	158.37	25.35	44.62	75.00	112.60	38.20
3	51 – 52	32.42	37.36	53.24	42.21	43.93	50.16	50.26	39.57
4	52 – 53	36.66	39.85	45.83	45.21	45.84	41.79	35.31	41.60
5	53 – 54	39.95	39.44	37.31	38.87	39.14	38.51	38.38	39.26
6	54 – 55	44.54	39.15	34.74	32.14	32.26	32.59	34.73	36.57
7	55 – 56	46.13	39.83	31.54	28.59	28.16	27.02	26.59	26.32
8	56 – 57	43.49	40.66	118.77	31.65	29.27	63.03	93.51	29.70
9	57 – 58	40.32	40.62	30.81	36.80	37.14	32.22	32.06	36.63
Starboard Area Stress Distribution									
No	Frame	Starboard SB – from Centre Line (Mpa)							
		T centre – L1 300 mm	L1 – L2 900 mm	L2 – L3 1500 mm	L3 – T Side 2100 mm	T side – L4 2700 mm	L4 – L5 3300 mm	L5 – L6 3900 mm	L6 – L7 4500 mm
1	49 – 50	12.57	18.87	16.80	14.19	13.64	19.89	19.44	23.14
2	50 – 51	38.22	135.18	94.20	43.47	25.85	152.82	26.25	30.67
3	51 – 52	39.94	53.87	39.97	45.69	42.03	77.98	37.489	32.62
4	52 – 53	40.94	35.97	45.60	45.74	44.15	45.75	38.51	36.74
5	53 – 54	39.02	38.52	38.66	38.81	38.87	37.00	39.25	39.74
6	54 – 55	36.20	34.98	32.65	31.47	32.33	34.81	39.11	44.34
7	55 – 56	26.65	28.42	26.69	28.19	28.26	30.79	39.79	46.06
8	56 – 57	28.30	130.37	88.86	29.25	31.49	93.25	39.76	43.41
9	57 – 58	36.55	30.88	29.50	37.11	36.85	34.21	43.06	40.42

4) Over Load Condition and Hogging Wave Condition

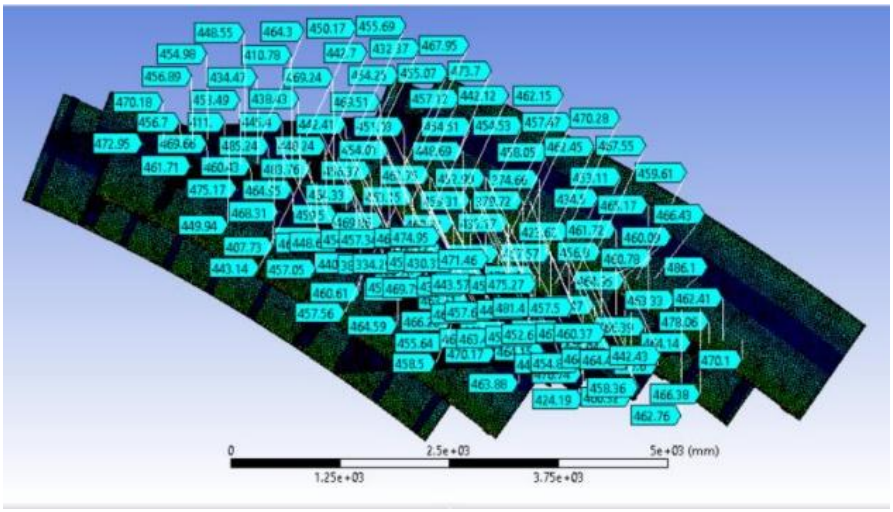

Figure. 22. Stress Distribution - *Over Load Condition and Hogging Wave Condition*

TABLE 10.
STRESS DISTRIBUTION OVERLOAD CONDITION AND HOGGING WAVE CONDITION

Port Side Area Stress Distribution									
No	Frame	Port Side PS – from Centre Line (Mpa)							
		L6 – L7 4500 mm	L5 – L6 3900 mm	L4 – L5 3300 mm	T side – L4 2700 mm	L3 – T Side 2100 mm	L2 – L3 1500 mm	L1 – L2 900 mm	T centre – L1 300 mm
1	49 – 50	472.95	470.18	456.70	456.89	454.98	449.94	448.55	464.30
2	50 – 51	461.71	469.43	411.00	453.49	434.47	407.73	410.78	443.14
3	51 – 52	475.17	460.43	485.24	445.40	438.43	457.05	469.24	454.25
4	52 – 53	468.31	464.95	483.76	448.24	442.41	460.61	469.51	457.56
5	53 – 54	470.17	459.50	464.33	456.37	454.01	451.03	454.51	462.71
6	54 – 55	440.91	469.86	464.59	463.15	462.75	455.64	448.69	458.5
7	55 – 56	466.30	460.76	460.12	460.83	459.31	452.99	433.17	379.72
8	56 – 57	466.26	463.51	485.15	460.02	463.88	471.25	457.57	432.62
9	57 – 58	470.17	462.67	480.15	464.15	462.73	470.74	471.47	465.04
Starboard Area Stress Distribution									
No	Frame	Starboard SB – from Centre Line (Mpa)							
		T centre – L1 300 mm	L1 – L2 900 mm	L2 – L3 1500 mm	L3 – T Side 2100 mm	T side – L4 2700 mm	L4 – L5 3300 mm	L5 – L6 3900 mm	L6 – L7 4500 mm
1	49 – 50	461.55	448.64	450.17	454.58	457.34	455.69	467.47	474.95
2	50 – 51	442.70	380.93	334.29	432.37	453.35	430.33	467.95	471.46
3	51 – 52	453.96	469.79	455.07	438.78	443.57	473.70	459.63	475.27
4	52 – 53	457.12	467.47	457.64	442.12	447.98	481.40	462.15	457.50
5	53 – 54	463.44	454.53	451.25	452.6	457.47	463.23	460.37	470.28
6	54 – 55	458.05	446.78	454.89	462.45	464.84	464.47	467.5	442.43
7	55 – 56	374.66	434.50	453.11	458.36	460.78	460.09	459.31	466.43
8	56 – 57	424.19	456.80	461.72	460.32	465.17	486.10	462.76	466.38
9	57 – 58	464.95	466.39	475.60	463.33	464.14	478.06	462.41	470.10

N. Maximum Stress Value and Location

Table 11 and the accompanying figures provide the maximum stress values and their respective locations.

TABLE 11.
MAXIMUM STRESS VALUE AND LOCATION

Maximum Stress Value and Location			
No	Condition	Stress Maximum	
		Stress (Mpa)	Location Stress
	Normal Load		
1	Sagging	126.2	Starboard – between Longitudinal 1 & 2 (900 from CL) – between Frame 56 & 57
2	Hogging	418.5	Starboard – between Longitudinal 4 & 5 (3300 from CL) – between Frame 56 & 57
	Overload		
1	Sagging	158.4	Portside – between Longitudinal 4 & 5 (3300 from CL) – between Frame 50 & 51
2	Hogging	486.1	Starboard – between Longitudinal 1 & 2 (900 from CL) – between Frame 56 & 57

O. Deformation

Deformation occurs when the stress value surpasses the material's allowable stress (yield strength). The yield strength specified for the material is 321 MPa, and the stress values are detailed in Table 11. The stress results indicate that in two conditions, the yield strength is exceeded: during normal loading, the hogging wave reaches 418.5 MPa, and under overload conditions, it reaches 486.1 MPa. Once the stress surpasses the yield strength, deformation occurs, leading to permanent changes in the material's shape (plastic deformation).

P. Fatigue Life

Based on the fatigue life calculation results in the table above using the Sonderberg method, there is a significant difference in the ship's lifespan depending on the load conditions. For instance, the ship's lifespan is approximately 400.6 years under normal load conditions, while under overload conditions with sagging, the lifespan is only around 126.2 years. Suppose the same load is applied continuously without any variation in the load. In that case, the lifespan for normal load hogging conditions is only 6.4 years, while for overload hogging conditions, the lifespan is reduced to 4.3 years.

This result shows that the ship's lifespan will be much shorter if it is continuously subjected to overload conditions or if the load cycle does not change. It indicates the need to reevaluate the design calculations and the ship's structural strength to ensure safe and effective operation over a longer period. The existing ship design must be reviewed to confirm that the ship's structure can withstand the loads under normal and overload conditions to prevent structural failure that could jeopardize the ship's operation.

Additionally, with the stress value reaching 418.5 MPa, which exceeds the Ultimate Tensile Strength (UTS) limit, there is a potential for material fracture. Stress exceeding the UTS limit can cause permanent deformation or catastrophic material failure, necessitating the ship's structural design adjustments to mitigate this risk. The vehicle load limits must also be evaluated to ensure that the transported cargo aligns with the ship's design capacity, avoiding structural damage that could shorten the ship's service life and endanger operational safety.

This study was conducted with measurements limited to the car deck area, specifically at the midship location. Therefore, a comprehensive review of the entire ship design, including other places, is necessary to ensure that the ship's structure can uniformly bear the loads and operate safely across all vessel parts.

TABLE 12.
FATIGUE LIFE CALCULATION

Load Input			
No	Condition	Sonderberg Method	
		Cycle	Years
	Normal Load		
1	Sagging	1692400000	400.6
2	Hogging	26936000	6.4
	Overload		
1	Sagging	533250000	126.2
2	Hogging	17996000	4.3

IV. CONCLUSION

Based on the analysis results, the highest stress value under hogging wave conditions exceeds the yield strength of 321 MPa. In normal loading and hogging wave conditions, the highest stress value of 486.1 MPa was found on the starboard side between longitudinal reinforcements 1 and 2 (900 mm from the centerline), between frames 56 and 57. A fatigue life of 4.3 years indicates that the car deck structure under these conditions has a limited lifespan when subjected to loads exceeding the design specifications. Loading beyond this limit will shorten the vessel's lifespan, necessitating a reevaluation of the structural design or regulatory measures regarding vehicle load restrictions, especially for heavy vehicles, to ensure the long-term safety and durability of the ship's structure.

ACKNOWLEDGEMENTS

The author would like to thank all individuals and institutions who indirectly supported this research through access to data, facilities,

and academic feedback.

REFERENCES

[1] Badan Pusat Statistik, Statistik Transportasi Laut, Badan Pusat Statistik, 2022. [Online]. Available: https://www.bps.go.id/id/publication/2023/11/27/945749d88a6234417d01c337/statistik-transportasi-laut-2022.html

[2] Komite Nasional Keselamatan Transportasi, Laporan Statistik Investigasi Kecelakaan Transportasi Tahun 2023 Semester 2, Komite Nasional Keselamatan Transportasi, 2023.

[3] Y. Denev, "Ship Causalities – Reasons and Statistical Analyze," TransNav, vol. 16, no. 4, pp. 607–610, 2022, doi: 10.12716/1001.16.04.01.

[4] F. P. Siswanto and I. Hamidah, "Perkembangan Informasi Geospasial Tematik Tema Transportasi Setelah Penetapan Kebijakan Satu Peta: Studi Kasus Tematik Kementerian Perhubungan," SNG, vol. 3, p. 117, Feb. 2019, doi: 10.24895/SNG.2018.3-0.935.

[5] Elizabeth, S. Cecilya, and S. Sunaryo, "Waste and hazardous material handling at green ship recycling facilities," Marit. Technol. Res., vol. 6, no. 3, p. 268423, 2024, doi: 10.33175/mtr.2024.268423.

[6] F. Kabakcioglu and E. Bayraktarkatal, "A Multihull Boat's Fatigue Analysis at Early Design Phase," JMSE, vol. 10, no. 5, p. 560, Apr. 2022, doi: 10.3390/jmse10050560.

[7] O. Ozguc, "Oil Tanker Simplified Fatigue Assessment with Inspection and Repair Approach and Parameters," Trans. Marit. Sci., vol. 10, no. 1, Apr. 2021, doi: 10.7225/toms.v10.n01.003.

[8] M. Marino et al., "Analysis on a database of ship accidents in port areas," Data in Brief, vol. 48, p. 109127, Jun. 2023, doi: 10.1016/j.dib.2023.109127.

[9] Corigliano, F. Frisone, C. Chianese, M. Altosole, V. Piscopo, and A. Scamardella, "Fatigue Overview of Ship Structures under Induced Wave Loads," JMSE, vol. 12, no. 9, p. 1608, Sep. 2024, doi: 10.3390/jmse12091608.

[10] M. N. Misbah, D. Setyawan, and W. M. Dananjaya, "Construction strength analysis of landing craft tank conversion to passenger ship using finite element method," J. Phys.: Conf. Ser., vol. 974, p. 012054, Mar. 2018, doi: 10.1088/1742-6596/974/1/012054.

[11] W. D. Yunanto, I. P. Mulyatno, and A. Trimulyono, "Analisa Kekuatan Konstruksi Car Deck pada Kapal 'Kapal ROPAX 5000GT' dengan Metode Elemen Hingga," 2016.

[12] E. C. Tupper, Introduction to Naval Architecture, 4th ed. Amsterdam: Elsevier, Butterworth-Heinemann, 2004.

[13] M. Shama, Buckling of Ship Structures. Berlin, Heidelberg: Springer, 2013, doi: 10.1007/978-3-642-17961-7.

[14] D. J. Eyres and G. J. Bruce, "Basic design of the ship," in Ship Construction, Elsevier, 2012, pp. 3–9, doi: 10.1016/B978-0-08-097239-8.00001-5.

[15] Biro Klasifikasi Indonesia, Rules for Structures (Vol. II), 2011.

A. Biran, Ship Hydrostatics and Stability. Oxford: Butterworth-Heinemann, 2003.

[16] Y. Okumoto, Y. Takeda, M. Mano, and T. Okada, Eds., Design of Ship Hull Structures. Berlin, Heidelberg: Springer, 2009, doi: 10.1007/978-3-540-88445-3.

[17] M. U. Pawara, A. Alamsyah, R. J. Ikhwani, A. R. Siahaan, and A. M. N. Arifuddin, "A Finite Element Analysis of Structural Strength of Ferry Ro-Ro's Car Deck," INVOTEK, vol. 22, no. 1, pp. 47–60, Jul. 2022, doi: 10.24036/invotek.v22i1.959.

[18] L. Zhang et al., "Methods for fatigue-life estimation: A review of the current status and future trends," Nanotechnology and Precision Engineering, vol. 6, no. 2, p. 025001, Jun. 2023, doi: 10.1063/10.0017255.

[19] ClassNK, Investigation Report on Structural Safety of Large Container Ships, 2014.

[20] C. Hibbeler, Mechanics of Materials, 8th ed. Pearson Prentice Hall, 2011.

[21] Liu, G. Feng, J. Wang, H. Ren, W. Song, and P. Lin, "Fatigue Life Assessment in the Typical Structure of Large Container Vessels Based on Fracture Mechanics," JMSE, vol. 11, no. 11, p. 2075, Oct. 2023, doi: 10.3390/jmse11112075.

[22] Budianto, "Analisis Fatigue pada Struktur Kapal Penangkap Ikan 30 GT," JK, vol. 9, no. 2, p. 137, Nov. 2016, doi: 10.21107/jk.v9i2.1590.

[23] N. Fatchurrohman and S. T. Chia, "Performance of hybrid nano-micro reinforced Mg metal matrix composites brake calliper: simulation approach," IOP Conf. Ser.: Mater. Sci. Eng., vol. 257, p. 012060, Oct. 2017, doi: 10.1088/1757-899X/257/1/012060.

[24] G. Budynas, Shigley's Mechanical Engineering Design, 9th ed., 2006.

[25] M. Barraza-Contreras, M. R. Piña-Monarrez, and A. Molina, "Fatigue-Life Prediction of Mechanical Element by Using the Weibull Distribution," Applied Sciences, vol. 10, no. 18, p. 6384, Sep. 2020, doi: 10.3390/app10186384.